

Supplemental information

**Novel requirements for HAP2/GCS1-mediated
gamete fusion in *Tetrahymena***

Jennifer F. Pinello, Josef Loidl, Ethan S. Seltzer, Donna Cassidy-Hanley, Daniel Kolbin, Anhar Abdelatif, Félix A. Rey, Rocky An, Nicole J. Newberger, Yelena Bisharyan, Hayk Papoyan, Haewon Byun, Hector C. Aguilar, Alex L. Lai, Jack H. Freed, Timothy Maugel, Eric S. Cole, and Theodore G. Clark

Figure S1. Sexual development in *Tetrahymena thermophila*. Related to Figure 1.

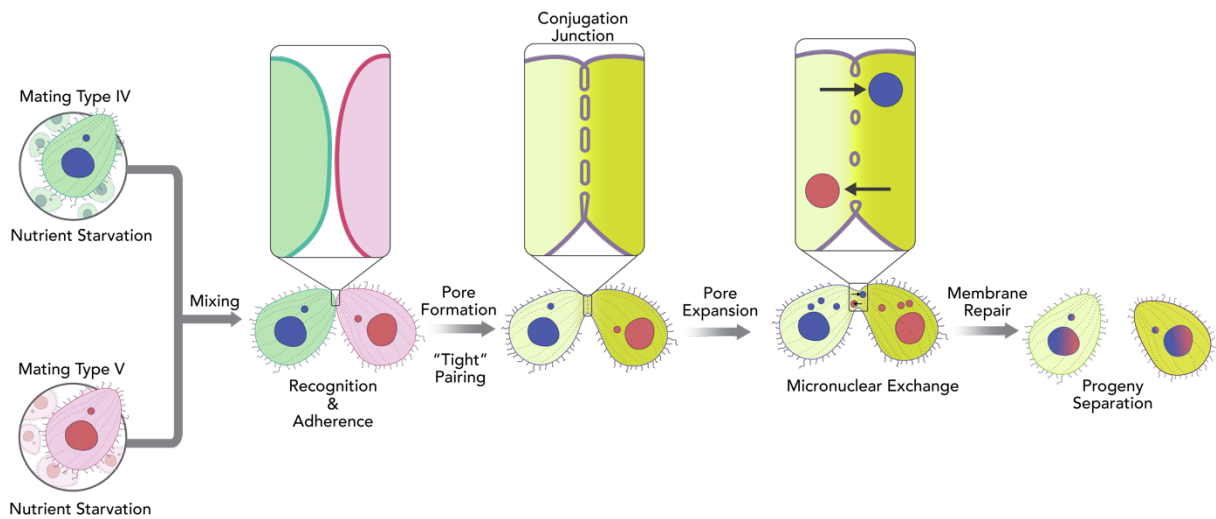


Figure S1. The sexual cycle of *T. thermophila* is shown from left to right beginning with **Nutrient starvation** to induce mating competence. For simplicity, only two mating types (IV and V) are shown. **Mixing:** Physical interactions between cells of complementary mating types lead to rapid upregulation of large numbers of genes^[S1–3] including those involved in mating type recognition, adherence, meiosis, and membrane pore formation. Roughly 30 min after mixing, cells form “loose” pairs consisting of both autologous and heterologous mating types. **Recognition and Adherence:** By 2 hr post-mixing (30°C), transient interactions between cells give way to “**Tight**” Pairing of heterologous mating types at a region of specialized membrane near the anterior of cells known as the conjugation junction. **Pore Formation:** The formation of mechanically stable, “tight” pairs coincides temporally with the formation of HAP2/GCS1-mediated fusion pores at the conjugation junction^[S4]. **Pore Expansion:** Over time, pores expand to form a lacey curtain or network of membranous tubules separating paired cells^[S5–7]. **Micronuclear Exchange:** In response to mating, germline micronuclei undergo meiosis to form 4 haploid pronuclei. Beginning roughly 5 hr post-mixing, one pronucleus from each cell migrates across the junction eventually fusing with a stationary pronucleus in the mating partner. The resulting zygotic (diploid) micronuclei then divide to give rise to new, transcriptionally active macronuclei, and silent germline micronuclei, with all other parental and unused meiotic nuclear products being degraded (details not shown). **Membrane Repair and Progeny separation:** When new macronuclear development is complete, membrane pores at the conjugation junction are repaired^[S8] and progeny cells separate (beginning ~12 hr post-mixing). **See also Figure 1.**

Figure S2. mRNA expression patterns and amino acid sequences of *GFU1* and *GFU2* coding regions. Related to Figures 1 and 3.

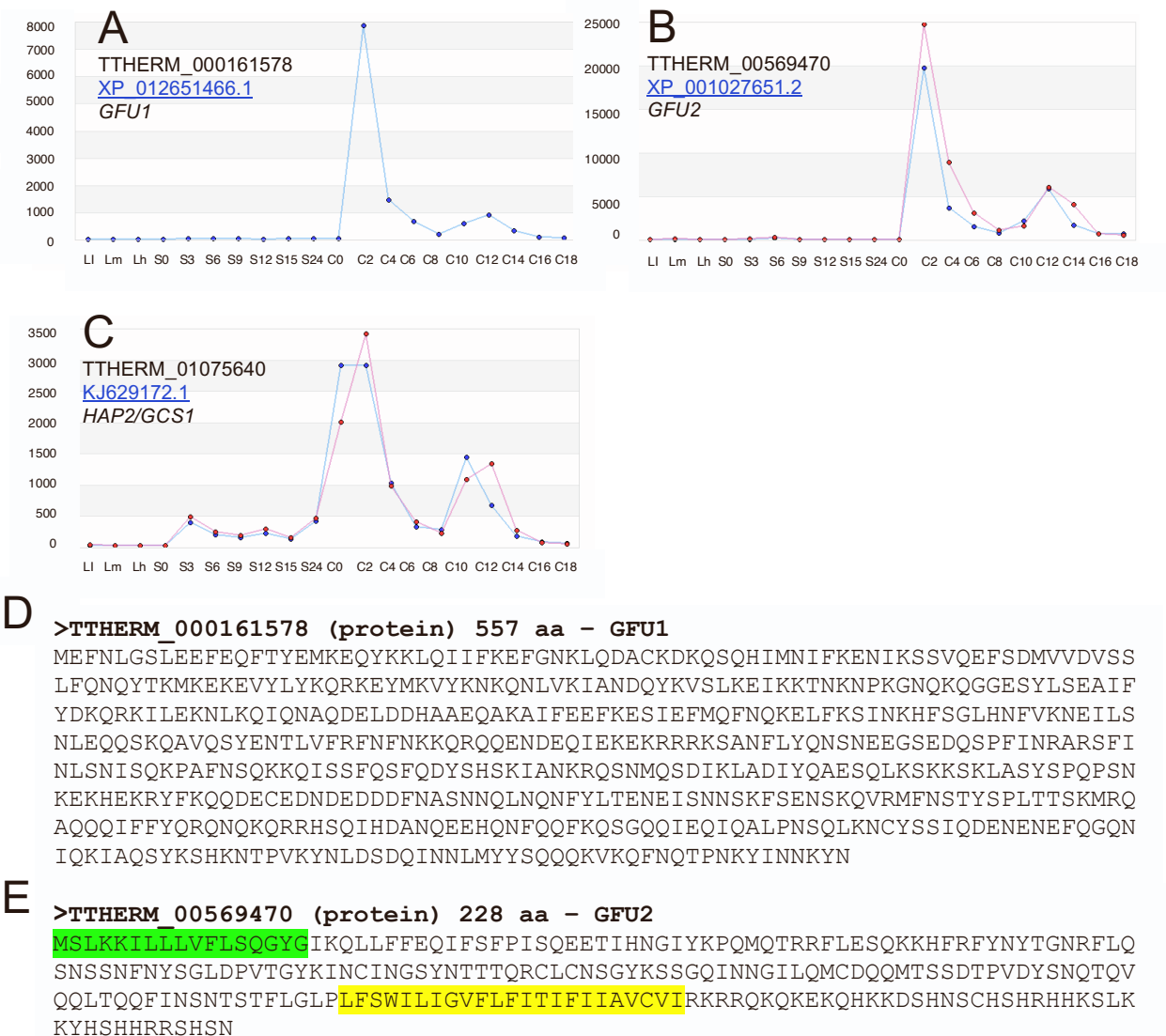


Figure S2. Panels (A-C) show screenshots of mRNA expression data for three genes upregulated during conjugation, namely, *GFU1* (A), *GFU2* (B), and *HAP2/GCS1* (C) from the *Tetrahymena Functional Genomics Database* (TetraFGD) (<http://tfgd.ihb.ac.cn/>). THERM gene identifiers from the *Tetrahymena Genome Database* (<https://tet.ciliate.org/>) and corresponding NCBI/GenBank (XP;KJ) accession numbers are listed in the upper left-hand corners of each panel. Note that the corresponding transcript ID for *GFU1* is denoted as gene_000009463 in the TetraFGD. All three genes show remarkably similar patterns of expression with transcript levels rising immediately upon mixing complementary mating types (C0 on the x-axis) and reaching a maximum at ~2 hr post-mixing (C2). Expression then falls to near baseline levels before rising again and forming smaller secondary peaks at ~12 hr post-mixing (C12). Developmental stages (L; S; and C) on the x-axis denote vegetative growth (L; Lm; Lh = low, medium and high cell density cultures); time after starvation (S0-24 hr); and time after mixing starved cultures of complementary mating types (C0-18 hr). Panels (D,E) show the deduced amino acid sequences of *GFU1* (D) and *GFU2* (E). *GFU1* localizes to the conjugation junction (see Fig. 3D-F) but is not predicted to be a transmembrane protein. *GFU2*, on the other hand, has all the hallmarks of a single-pass transmembrane protein with predicted signal peptide and transmembrane helices highlighted in green and yellow, respectively (see also, Fig. 3C). See also Figs. 1 and 3.

Figure S3. AlphaFold2 prediction of GFU2 structure. Related to Figure 3.

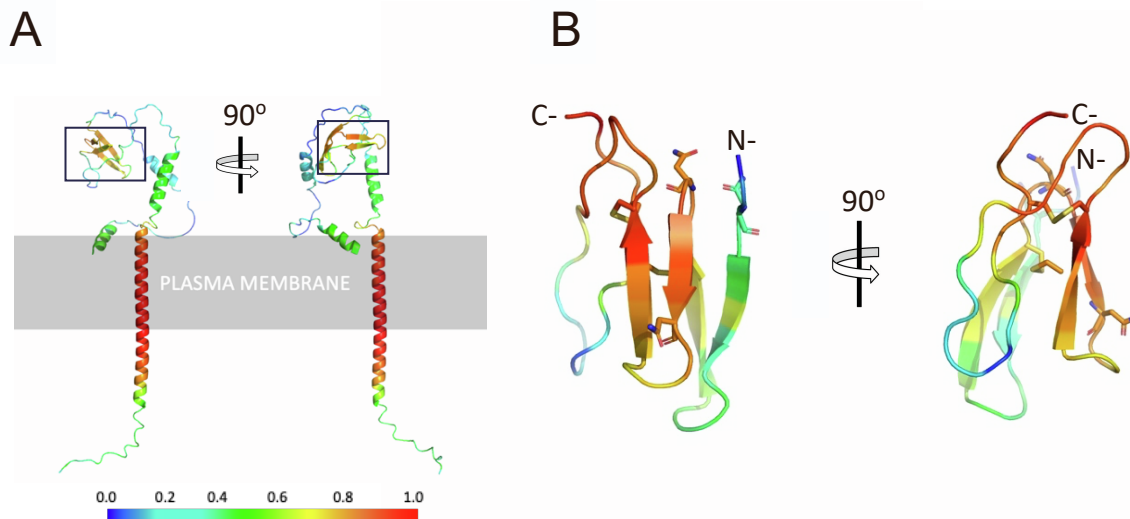


Figure S3. Panel (A) shows orthogonal views of a predicted structure of GFU2 (residues 18-228) based on AlphaFold2 as it would appear in the plasma membrane (gray bar) with the N-terminal extracellular domain at the top. Note that the α -helix at the N-terminus is aliphatic and probably lies flat on the membrane rather than penetrating it as shown. Color coding is based on prediction reliability scores (pLDTT²⁸) with blue (0.0) representing the lowest and red (1.0) the highest confidence scores. Aside from the transmembrane helix (residues 164-186), the only region with homology to other proteins in the PDB database contains two sets of antiparallel β -sheets stabilized by disulfide bonds (Cys93-Cys105 and Cys107-Cys125). This region (residues 77-129) is outlined by the boxes in panel (A) and is expanded in the orthogonal views in panel (B). N- and C- represent the N-terminal and C-terminal ends of the fragment. **See also Figs. 3.**

Figure S4. Lipid mixing assays with recombinant GFU1. Related to Figure 3.

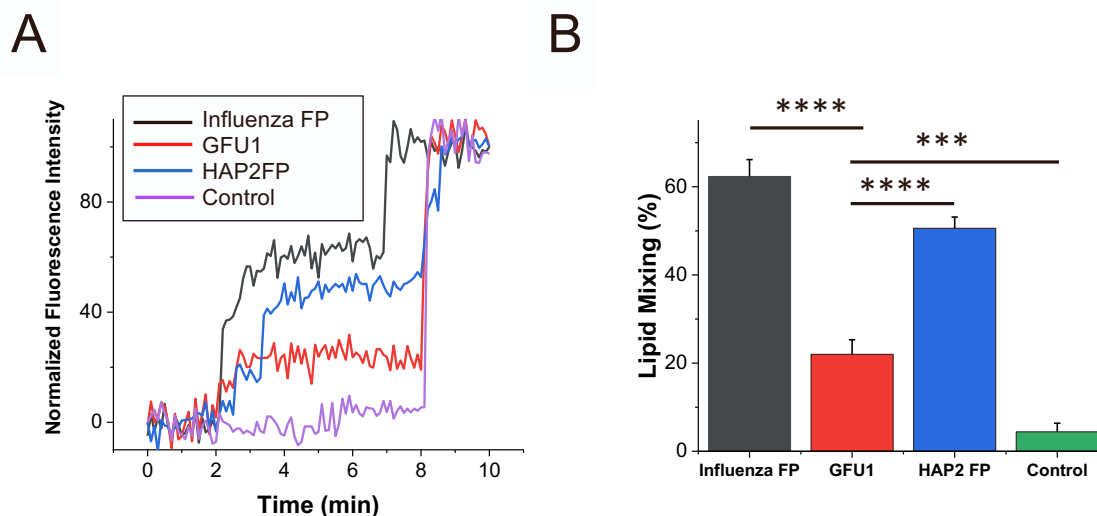


Figure S4. Panels (A) and (B) show the results of lipid mixing experiments comparing recombinant GFU1 with fusion peptides from influenza HA, *Tetrahymena* HAP2/GCS1, and a scrambled HAP2 fusion peptide used in electron spin resonance studies (Fig. 3F,G). Protein moieties were added to a mixed population of unlabeled and R18-quenched liposomes at ~2 min, followed by addition of Triton X-100 at 7–8 min to establish maximum dequenching values for normalization purposes (final intensity = 100%). Results from a representative experiment are shown in panel (A). Panel (B) shows the mean normalized percent lipid mixing from 3 independent experiments. As expected, fusion peptides from influenza HA and *Tetrahymena* HAP2/GCS1 promoted rapid merger of membrane vesicles as shown in panel (A). Lower but significant levels of membrane mixing were also observed with GFU1 as indicated in panel (B). All measurements were made at 25°C with membrane compositions consisting of POPC:POPG:Chol=5:2:3. Error bars show the standard deviation for each group. A non-parametric ANOVA analysis was conducted to determine statistical significance between groups (**** = $p < 0.0001$; *** = $p < 0.001$). **See also, Figure 3.**

Figure S5. Serial sections through the conjugation junction of *Tetrahymena* wild type mating pairs. Related to Figure 6.

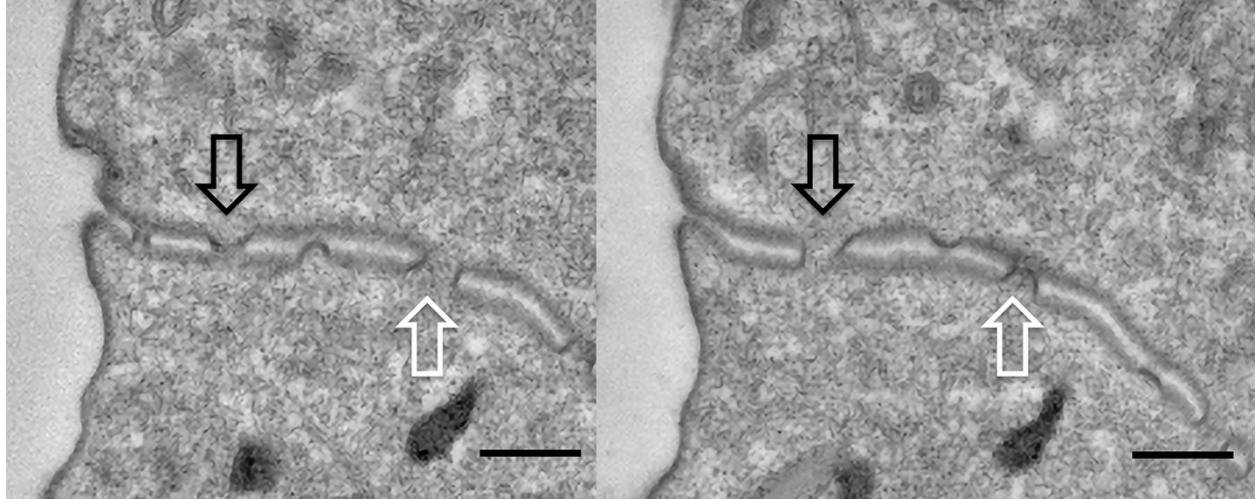


Fig. S5. Wild type *T. thermophila* mating pairs (CU428.2 X SB1969) were harvested at 4 hr post-mixing and prepared for conventional thin-section transmission electron microscopy using chemical fixation as previously described⁶. The left and right-hand panels show adjacent (90 nm) sections through the conjugation junction of a single mating pair with cells oriented top-to-bottom as in Fig. 6. Pores are visible along the length of the junction. In the left-hand panel, the black arrow indicates a dome-shaped structure protruding from the cell on top, while the white arrow, shows a fully open pore. In the adjacent section (right-hand panel), an open pore is present where the dome-shaped structure appeared in the adjacent section (black arrow). Conversely, a dome-shaped structure appears to be protruding from the cell on the bottom in the same position as the open pore in the adjacent section on the left (white arrow). Scale bar in the lower right corner of each panel = 0.5 μm . **See also, Fig. 6.**

Table S1. PCR Primers, related to STAR Methods.

Primer Name	Sequence 5' → 3'	Use
#1	AAGAGGTAGTAGCTTATTGTTG	GFU1 strain construction
#2	TTCCTCTTAATTAGCATCATGG	GFU1 strain construction
#3	TAGATGATCATGCAGCGG	GFU1 KO validation
#4	CACTACCTTCCTCATTGC	GFU1 KO validation
#5	ACTAAAGGGAACAAAAGCTGGAGCTCGCTTTTTCTATCAAGTCTTAAATG	GFU2 strain construction
#6	ACCCGTCAGGTGCCTGGTACTGCAGCTTAAGGTGAGAAATATTAAATTGC	GFU2 strain construction
#7	ACGTCGCACCATGTGACCTCGAGATGGTACACTCAAATTTGTGC	GFU2 strain construction
#8	CTCACTATAGGGCGAATTGGGTACCTTAGTAAGTAGCTAATATGTCCC	GFU2 strain construction
#9	GTTTTCTATTAGTTAAGAAGAAAC	GFU2 KO validation
#10	TGTATTGTAAGAGCCGTTTATACAG	GFU2 KO validation
N7_R164A_F	TGATCTATCAGCTGGTAAAGTGTGCTATGC	R164A strain construction
N7_R164A_R	TTACCCATGCCTAATATATC	R164A strain construction
5'FW	TGATGGCGATGAATGAACACTGAGCTTGCTTCTTATTCACCTC	GFU1-HA & GFU1-mCherry strain constr.
5'RV_mCherry	ATCTTCTTCTCCTTTTGAACCATATTGTATTTATTATTAATGTATTTATTTGGAGTC	GFU1-mCherry strain constr.
5'RV_HA	GCATAATCAGGAACATCATAAGGATAATTGTATTTATTATTAATGTATTTATTTGGAGTC	GFU1-HA strain constr.
3'FW	CCCGGGGGATCTGAATTCGATATCAAGCTTTTTGCGCTAATGCATAGAAC	GFU1-HA & GFU1-mCherry strain constr.
3'RV	GCGAGCACAGAATTAATACGACTGAGTGGATTTTGATGCAAGG	GFU1-HA & GFU1-mCherry

		Strain constr.
BamHI-mcherry_Fw1	ATGGTTTCAAAGGAGAAGAAGATAAC	GFU1-mCherry strain constr.
BamHI-HA_Fw1	TATCCTTATGATGTTCCCTGATTATGC	GFU1-HA strain constr.
HindIII-Neo4-RV2	AAGCTTGATATCGAATTCAGATCC	GFU1-HA & GFU1-mCherry strain constr.
5'RACE-Outer	TGATGGCGATGAATGAACACTG	GFU1-HA & GFU1-mCherry Strain constr.
3'RACE-Outer	GCGAGCACAGAATTAATACGACT	GFU1-HA & GFU1-mCherry strain constr.

References to Supplementary Material.

- S1. Xiong, J., Lu, Y., Feng, J., Yuan, D., Tian, M., Chang, Y., Fu, C., Wang, G., Zeng, H., and Miao, W. (2013). Tetrahymena functional genomics database (TetraFGD): an integrated resource for Tetrahymena functional genomics. *Database (Oxford) 2013*, bat008. <https://doi.org/10.1093/database/bat008>.
2. Pinello, J.F., and Clark, T.G. (2022). HAP2-Mediated Gamete Fusion: Lessons From the World of Unicellular Eukaryotes. *Front. Cell Dev. Biol. 9*, 807313. <https://doi.org/10.3389/fcell.2021.807313>.
3. Cole, E.S. (2016). Cell-Cell Interactions Leading to Establishment of a Mating Junction in Tetrahymena and Paramecium, Two “Contact-Mediated” Mating Systems. In *Biocommunication of Ciliates*, G. Witzany and M. Nowacki, eds. (Springer International Publishing), pp. 195–220. https://doi.org/10.1007/978-3-319-32211-7_12.
4. Pinello, J.F., Lai, A.L., Millet, J.K., Cassidy-Hanley, D., Freed, J.H., and Clark, T.G. (2017). Structure-Function Studies Link Class II Viral Fusogens with the Ancestral Gamete Fusion Protein HAP2. *Current Biology 27*, 651–660. <https://doi.org/10.1016/j.cub.2017.01.049>.
5. Wolfe, J. (1982). The conjugation junction of Tetrahymena: Its structure and development. *J Morphol 172*, 159–178. <https://doi.org/10.1002/jmor.1051720204>.
6. Cole, E.S., Giddings, T.H., Ozzello, C., Winey, M., O’Toole, E., Orias, J., Hamilton, E., Guerrier, S., Ballard, A., and Aronstein, T. (2015). Membrane dynamics at the nuclear exchange junction during early mating (one to four hours) in the ciliate Tetrahymena thermophila. *Eukaryot Cell 14*, 116–127. <https://doi.org/10.1128/EC.00164-14>.
7. Cole, E.S. (2000). The Tetrahymena Conjugation Junction.
8. Cole, E.S., Dmytrenko, O., Chmelik, C.J., Li, M., Christensen, T.A., Macon, E.P., Nilsson, H.J., Blower, R.J., Reuter, T.G., Beckman, J.P., et al. (2018). Restoration of cellular integrity following “ballistic” pronuclear exchange during Tetrahymena conjugation. *Dev Biol 444*, 33–40. <https://doi.org/10.1016/j.ydbio.2018.09.019>.